ELSEVIER

International Journal of Mass Spectrometry 201 (2000) 69–85

International Journal of Mass Spectrometry

Structures and reactivity of gaseous glycine and its derivatives

Bülent Balta[a], Maral Basma[a], Viktorya Aviyente[a], Chuanbao Zhu[b], Chava Lifshitz[b,1,*]

[a]*Chemistry Department, Boğaziçi University, 80815, Bebek, Istanbul, Türkiye*
[b]*Department of Physical Chemistry and the Farkas Center for Light Induced Processes, The Hebrew University of Jerusalem, 91904, Jerusalem, Israel*

Received 9 September 1999; accepted 11 November 1999

Abstract

B3LYP/6-31++G** has been used to model the conformers of glycine, protonated glycine, the unimolecular fragmentation, the proton transfer and the bimolecular proton exchange reactions with NH_3. B3LYP/6-31++G** has located all the conformers—except one—located previously with electron correlation methods. The results show that the performance of B3LYP/6-31++G** is significantly better than that of the HF method and in most cases as good as the ab initio theories such as MP2, CCSD, and CISD. We have thus used B3LYP/6-31++G** in order to understand the unimolecular fragmentation and bimolecular reactions of glycine with NH_3. The proton has been found to be mobile over all basic sites when a threshold of ~33 kcal/mol is reached. A barrier of ~50 kcal/mol exists for the fragmentation reaction, H_2O and CO being sequentially eliminated. The amino protons are exchanged with an onium mechanism and the carboxylic proton is exchanged via a salt bridge complex. (Int J Mass Spectrom 201 (2000) 69–85) © 2000 Elsevier Science B.V.

Keywords: Protonated glycine; DFT; Conformers; H/D exchange; Potential energy profiles; Proton migration; Fragmentation

1. Introduction

The investigation of protonated peptides by mass spectrometry is of increasing importance [1–8]. The fragmentation pattern allows the determination of the amino acid sequence of a given peptide. H/D exchange reactions of protonated species with deuterated bases in the gas phase provide insight into the number of active hydrogens available for exchange in a given conformation. As the simplest amino acid, glycine and its oligomers are of special interest. Previous H/D exchange reactions of protonated glycine and polyglycines were carried out under low pressures [2,4]. Recent experiments at high pressure using electrospray ionization combined with a flow tube provided clear evidence concerning the existence of collision complexes in the reaction of protonated diglycine $(Gly)_2H^+$ with ND_3 [1]. All the five labile hydrogens of protonated diglycine can be exchanged, whereas the reaction efficiency for the exchange of the first three was found to be higher than for the last two [1].

Further information about the structure and fragmentation pattern of peptides can be obtained via quantum chemical calculations. The large molecular size of peptides restricts high level ab initio calcula-

* Corresponding author.
[1] Archie and Marjorie Sherman Professor of Chemistry.

PII S1387-3806(00)00218-9

tions to monomeric units, i.e. amino acids. Low level ab initio calculations (Hartree-Fock) were carried out on monoglycine [8,9], diglycine [8], triglycine [10], and semiempirical calculations up to pentaglycine [2]. On the other hand, Schäfer and co-workers insisted on the importance of the geometry optimization at the correlated levels and suggested that this might be crucial for theoretical investigations on polypeptides [11,12]. To the best of our knowledge, there is no correlated level optimization for diglycine, the simplest peptide, in the literature. As they mention in their article, the semiempirical study of Campbell et al. [2] fails to predict the correct order of basicity between glycine and NH_3. It was found that, for glycine and protonated glycine, Hartree-Fock (HF) theory gave geometries different than those obtained at higher levels [13,14]. Therefore, single point calculations based on HF structures may suffer from incorrect geometries. On the other hand, recent improvements in density functional theory (DFT) [15,16] provide a reasonable balance between the computational cost and accuracy of the results. However, to our knowledge, the only DFT work [17] that appeared in the literature provides only single point DFT energies based on low level optimized structures. Our ultimate goal in this series of papers, is to obtain the most important diglycine and protonated diglycine conformers and the mechanism of the H/D exchange reactions with ND_3.

In the first article, we restrict our scope to the structure of monoglycine, protonated monoglycine, and their reactions. There are two reasons for choosing monoglycine as the starting point. First of all, the quality of our calculations needs to be tested. Monoglycines have been extensively studied both theoretically [8,9,13,14,18–21] and experimentally [4,22–25] whereas data about diglycines are rare in the literature. Second, H/D exchange reactions of monoglycines were not studied by correlated methods. Therefore, an accurate modeling of these reactions may be highly instructive in the study of the diglycines.

We have started by exploring the conformational space of glycine. The second part of this paper is based on the N and O protonated structures of glycine. The third part concentrates on the unimolecular reactions of protonated glycine (intramolecular proton migration and fragmentation); the last part focuses on the bimolecular reactions between NH_3 and protonated glycine. Our next article will deal with modeling $(Gly)_2$, $(Gly)_2H^+$, and the H/D exchange reactions of $(Gly)_2H^+$ with ND_3.

2. Methods

All density functional calculations have been carried out using the GAUSSIAN 94 [26] package running on a DEC Alpha 233/4 and a DEC Alpha 433 at the Chemistry Department, Boğaziçi University. Preliminary semiempirical calculations using the PM3 [27] model were performed using Spartan [28].

All density functional calculations employed the Becke 3-parameter-Lee-Yang-Parr (B3LYP) [15,16] exchange–correlation functional that combines the Becke 3-parameter hybrid exchange functional with the gradient-corrected correlation functional of Lee, Yang, and Parr. Barone et al. [19] used various DFT methods including LDA, BLYP, and B3LYP for neutral glycine conformers and showed that only B3LYP gave the correct order of stability. Frequencies were calculated for all the stationary geometries. Real vibrational frequencies confirmed the presence of minima on the potential energy surface (PES), one imaginary frequency for the bond of interest indicated the existence of a transition state. Thermal energy contributions were evaluated at 298.15 K. In this text thermal energy will refer to the total (electronic, vibrational, translational, and rotational) energy of the system at 298.15 K. It was shown in the literature that for some small H-bonded dimers at least the 6-31+G** basis set had to be used in conjunction with the B3LYP method [29]. After some preliminary studies which had indicated the necessity of using diffuse and polarization functions, the 6-31++G** basis set was selected for this study. Tables 1 and 2 contain the geometrical parameters and energetics obtained in this study for the conformers of glycine. Tables 3–5 display the geometrical parameters and energetics, respectively, for the conformers of protonated glycine. Fig. 1 displays the conformers of glycine. Fig. 2(a) and (b) show respectively the N and

Table 1
Geometrical parameters for the glycine conformers; bond lengths are in angstroms and angles are in degrees

	Ip	IIn	IIIn	IVn	Vn	VIp	VIIIn
r(N–C)	1.449	1.470	1.451	1.455	1.461	1.447	1.453
r(C–C)	1.525	1.538	1.528	1.513	1.516	1.536	1.525
r(C=O)	1.213	1.209	1.213	1.213	1.212	1.206	1.206
r(C–O)	1.356	1.341	1.357	1.354	1.357	1.363	1.359
r(O–H)	0.973	0.987	0.973	0.973	0.972	0.969	0.969
A(N–C–C)	115.86	111.36	119.28	110.33	112.63	115.87	110.30
A(C–C–O)	111.53	113.98	113.50	111.87	112.23	115.49	115.96
A(C–C=O)	125.71	122.55	124.02	125.16	125.05	124.35	123.68
A(C–O–H)	107.5	105.35	106.84	107.27	107.27	111.16	111.13
A(H–N–C)	110.69	112.71	111.33	111.45	111.21	110.43	109.85
		112.89		110.54	110.54		111.90
A(H–N–H)	106.49	108.25	107.14	108.99	108.23	106.28	109.17
A(H–C–H)	105.62	106.68	105.46	106.50	107.09	106.12	106.67
D(O–C–C–N)	180	4.18	−0.06	161.25	−37.11	180	161.79
D(O=C–C–N)	0	183.66	179.93	−21.04	146.08	0	−20.98
D(H–O–C–C)	180	−0.89	179.99	176.86	−179.53	0	−6.02
D(H–N–C–C)	−58.92	−125.75	−59.75	161.42	60.07	−58.63	31.72
	58.92	111.20	59.74	40.06	180.31	58.63	153.14
OH----O	2.307		2.292	2.304	2.301		
OH----N		1.920					
NH----O–C			2.734		2.456		
			2.733		3.699		
NH----O=C	2.838			2.403		2.812	2.304
							3.650

O protonated conformers of glycine. The intramolecular proton migration reaction is depicted in Fig. 3(a) and (b). Fig. 3(c), (d), (e), and (f) illustrate the unimolecular fragmentation reactions. Fig. 4(a)–(f) exhibit the bimolecular reactions of protonated glycine.

3. Results and discussion

The discussion of the results focuses mainly on four different topics: neutral glycines, protonated glycines, the unimolecular fragmentation reaction and the bimolecular reaction mechanism.

Table 2
Electronic energies (E_{el}), total energies ($E_{el+thermal}$) at 298.15 K, zero point energies (ZPE) in hartrees and dipole moments (debye) of the conformers of glycine; values in parantheses are relative energies in kcal/mol

	Ip	IIn	IIIn	IVn	Vn	VIp	VIIIn
E_{el}	−284.456 874	−284.456 245	−284.454 479	−284.454 367	−284.452 530	−284.447 715	−284.445 106
	(0) (0)[a] (0)[b]	(0.39)	(1.50)	(1.57)	(2.73)	(5.75)	(7.39)
		(0.53)[a]	(1.44)[a]	(1.26)[a]	(2.20)[a]	(5.70)[a]	(7.08)[a]
		(2.9)[b]	(1.9)[b]	(2.2)[b]	(3.1)[b]	(7.0)[b]	(9.3)[b]
$E_{el+thermal}$	−284.371 544	−284.370 691	−284.369 112	−284.369 212	−284.367 242	−284.362 677	−284.360 252
	(0)	(0.54)	(1.53)	(1.46)	(2.70)	(5.56)	(7.09)
ZPE	0.079 677	0.080 033	0.079 688	0.079 547	0.079 710	0.079 294	0.079 153
Dipole moment	1.217	5.906	1.943	2.170	2.540	3.168	4.426

[a] MP2/6-311++G** energies of [20].
[b] HF/6-31G* energies of [9].

Table 3
Geometrical parameters for the N-protonated glycine conformers; bond lengths are in angstroms and angles are in degrees

	$1m(C_1)$	$2m(C_1)$	$3n(C_s)$
r(N–C)	1.510	1.516	1.508
r(C–C)	1.531	1.528	1.545
r(C=O)	1.215	1.197	1.212
r(C–O)	1.318	1.351	1.320
r(O–H)	0.976	0.976	0.971
r(N–H)	1.024	1.027	1.024
	1.024	1.027	1.024
	1.046	1.027	1.052
A(N–C–C)	105.60	112.27	104.95
A(C–C–O)	111.80	110.96	118.44
A(C–C=O)	120.60	122.11	118.66
A(C–O–H)	110.72	109.85	115.11
A(H–N–C)	105.12	111.15	103.77
	112.94	111.46	113.19
	112.94	111.10	113.19
A(H–N–H)	108.87	106.29	109.18
	108.87	108.31	109.18
	107.96	108.35	108.16
A(H–C–H)	108.86	108.91	109.19
D(O–C–C–N)	179.99	0.64	180
D(O=C–C–N)	−0.01	180.57	0
D(H–O–C–C)	179.99	179.89	179.99
D(H–N–C–C)	−118.59	−58.58	−118.55
	118.59	59.55	118.59
	0.02	180.47	0.02
OH----O	2.405	2.402	
NH----O–C		2.517	
		2.494	
NH----O=C	1.906		1.829

3.1. Neutral glycines

Glycine is the simplest amino acid existing in zwitterionic form, $^{+}H_3NCH_2COO^{-}$, in the crystal structures and in solution. In the gas phase, it exists in a non-ionized form. In Fig. 1, gas phase conformers of glycine deduced by Császár [20] are presented. The subscripts *p* and *n* stand for planar and nonplanar according to C_s or C_1 symmetries, respectively. The effort to determine the gas phase structure of glycine has an interesting history. The first microwave spectroscopic results by Suenram and Lovas [22a] and Brown et al. [23a] identified conformer IIp (Fig. 1) as the only gas phase conformer in conflict with ab initio calculations. The problem was solved when theoretical studies indicated that IIp had a much larger dipole moment than all the other conformers [22b]. Since microwave intensities depend on the dipole moment, IIp masked the other conformers in the spectrum. A few years later, Suenram and Lovas observed the microwave spectrum of Ip [22c]. Since then many computational results at the HF [9], MP2 [20], CISD [13], CCSD [13], and DFT [19] levels of theory appeared in the literature predicting up to eight conformers. At the HF and MP2 levels five of these conformers were found to exist at a considerable amount at room temperature. Godfrey and Brown [23b] used jet spectroscopy to observe the theoretically predicted conformers but they only found Ip and IIp to be present. They attributed this fact to the relaxation of high-energy conformers to more stable species and confirmed their approach with a theoretical investigation [30]. Although IR spectroscopy is very sensitive to intramolecular H bonding, and can therefore be used to identify different conformers, it is not practically possible to obtain a concentration of glycine in the gas phase sufficient to register its IR spectra. Adamowicz and co-workers [25] took the IR spectra of glycine and its deuterated derivatives isolated in low temperature argon matrices. Although at higher temperatures only Ip and IIp were observed, additional bands appeared in the IR spectra for samples deposited at temperatures below 13 K. Comparing these bands with theoretically predicted IR frequencies they could identify conformer IIIp that was converted to Ip above 13 K. They also found that the B3LYP/aug-cc-pVDZ method yielded vibrational frequencies similar to MP2 for glycine. Iijima and co-workers [24] showed with electron diffraction experiments that 76% of the gaseous glycine existed as Ip whereas the rest was a mixture of IIp and IIIp at 219 °C.

The potential energy surface depends significantly on the theoretical method of choice. The energy gap between Ip and IIp was observed to be 1.4 ± 0.4 kcal/mol in microwave spectroscopy [22] and 1.3–1.6 kcal/mol in IR experiments [31]. The same energy gap was predicted to be about 2–3 kcal/mol with HF theory using different basis sets [9,13]. Although simpler DFT methods like LDA and BLYP identified IIn as the most stable conformer, the use of the hybrid B3LYP functional restored the correct order with an

Table 4
Geometrical parameters for the O-protonated glycine conformers; bond lengths are in angstroms and angles are in degrees

	H5(C_s)	4n(C_s)	5m(C_1)	6m(C_1)	7m(C_s)	8m(C_s)
r(N–C)	1.462	1.424	1.416	1.439	1.427	1.416
r(C–C)	1.528	1.520	1.524	1.515	1.516	1.520
r(C–O[a])	1.260	1.274	1.278	1.285	1.281	1.283
r(C–O)	1.287	1.294	1.293	1.294	1.292	1.289
r(O–H)	0.975	0.977	0.977	0.976	0.977	0.978
r(O–H[a])	1.051	0.981	0.981	0.980	0.977	0.977
r(N–H)	1.017	1.011	1.012	1.011	1.011	1.011
A(N–C–C)	104.79	113.02	118.19	108.71	113.05	118.31
A(C–C–O)	125.92	123.07	123.96	125.18	116.17	116.95
A(C–C–O[a])	115.86	119.84	119.16	117.97	119.24	118.62
A(C–O–H)	114.55	114.73	114.73	114.53	118.13	118.51
A(C–O[a]–H)	101.33	113.66	114.02	114.06	117.54	117.86
A(H–N–C)	113.49	115.26	116.63	117.23	114.71	117.06
				118.35		
A(H–N–H)	108.71	111.47	112.63	113.98	110.83	113.03
A(H–C–H)	107.62	105.39	105.38	108.42	104.61	104.49
D(O–C–C–N)	180	180	179.99	90.89	180	180
D(O[a]–C–C–N)	0	0	0	−82.29	0	0
D(H–O–C–C)	0	0	0	10.02	180	180
D(H–O[a]–C–C)	0	180	179.99	172.69	180	180
D(H–N–C–C)	−117.61	−113.96	−68.57	−71.92	−115.01	−69.49
	117.61	113.96	68.57	70.94	115.01	69.49
OH----O[a]					2.487	2.491
O[a]H---O		2.271	2.277	2.278	2.474	2.479
O[a]H---N	1.653					
NH----O[a]–C			2.947			2.952
			2.947			2.952

[a] Oxygen atom at the syn position with respect to the amino group.

energy gap of 0.25 kcal/mol with a TZ2P basis set [19]. Perturbation methods for electron correlation yielded values of about 0.5 kcal/mol [20,21]. Higher correlation methods (CISD, CCSD) brought this value close to the experimental result [13]. In general, this value increases with a better treatment of the electron correlation and decreases with the size of the basis set. Hagler [32] suggested the experimental value to be revised and proposed a value of 1 kcal/mol. A balance between the stabilizing effect of different types of H-bonding (depicted in Scheme 1) and repulsive steric interactions [13,19,20] was used to explain the relative stabilities of the glycine conformers. The relative stabilities of the conformers other than Ip and

Table 5
Electronic energies (E_{el}), total energies ($E_{el+thermal}$) at 298.15 K, zero point energies (ZPE) in hartrees of the conformers of protonated glycine. Values in parantheses are relative energies in kcal/mol.

	1m(C_1)	2m(C_1)	3n(C_s)	H5(C_s)	4n(C_s)	5m(C_1)	6m(C_1)	7m(C_s)	8m(C_s)
E_{el}	−284.807 184	−284.799 710	−284.793 548	−284.782 0.16	−284.765 862	−284.765 209	−284.763 912	−284.759 671	−284.758 094
	(0.00)	(4.69)	(8.56)	(15.79)	(25.93)	(26.34)	(27.15)	(29.81)	(30.80)
	(0.00)[a]	(3.53)[a]	(9.12)[a]		(28.46)[a]	(29.05)[a]	(30.39)[a]	(32.66)[a]	(34.00)[a]
E_{el+th}	−284.707 345	−284.699 598	−284.694 237	−284.684 692	−284.668 529	−284.667 913	−284.666 248	−284.662 645	−284.661 293
	(0.00)	(4.86)	(8.23)	(14.22)	(24.36)	(24.74)	(25.79)	(28.05)	(28.89)
ZPE	0.094 262	0.094 271	0.093 705	0.092 031	0.091 063	0.091 406	0.091 751	0.090 816	0.090 822

[a] MP2/6-311+G** results from [14].

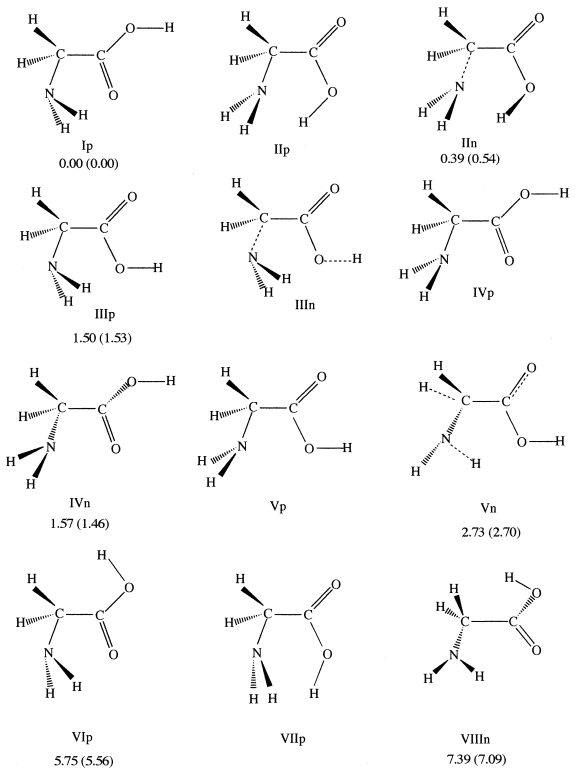

Fig. 1. Conformers of neutral glycine; electronic energies and total energies at 298.15 K (including zero point energies) are indicated below the structures as $E_{el}(E_{el+thermal})$ in kcal/mol relative to the most stable conformer Ip.

IIn or IIp are in reasonable agreement among different methods. It was assumed therefore that the main effect of the electron correlation was in the treatment of N . . . HO type of H bonding encountered only in IIn and IIp. Another conflict between theory and experiment is concerned with the symmetry of the second most stable conformer. Although calculations identified IIn (C_1) as a minimum and IIp (C_s) as a saddle point [13,19,20], experiments indicated a C_s symmetry for this conformer [23b]. It was pointed out that the zero point energy of the C_1 species exceeded the barrier (corresponding to the transition structure IIp) between IIn and its mirror image. Therefore, the most probable C_s geometry was observed in the experiment during this large amplitude vibration [23b]. The same situation is also predicted for IIIn [20].

Seven conformers of glycine (Ip, IIn, IIIn, IVn, Vn, VIp, VIIIn) were located in our calculations as minima on the potential energy surface of glycine, using B3LYP/6-31++G** (Fig. 1). Their geometrical parameters are presented in Table 1 and the relative energies of these species are presented in Table 2. For comparison MP2/6-311++G** [20] and HF/6-31G* [9] energies are also given in the same table. Hydrogen bridges occurring in different conformers of glycine can be classified in the following four classes (Scheme 1): (1) syn carbonyl functional group, (2) hydrogen bonding between the nitrogen lone pair and the carboxylic hydrogen resulting in a five membered ring, (3) bifurcated arrangement between the hydrogen atoms on the amino group and the oxygen atom on the carbonyl group, (4) bifurcated arrangement between the hydrogen atoms on the amino group and the oxygen atom on the hydroxyl group.

In the most stable conformer of neutral glycine, Ip (C_s), the N–H bonds are symmetrically oriented with respect to the carbonyl oxygen forming a bifurcated hydrogen bond. The non-planar conformer In (C_1) is almost isoenergetic ($+1.88 \times 10^{-4}$ kcal/mol) with Ip (C_s). Rauk and co-workers [18] pointed out that the stability of conformer Ip was not due to the bifurcated hydrogen bonding as shown by the extended value of the NCC angle and the H . . . O non bonded distance which is outside the van der Waals separation. On the other hand, the explanation of the stability of this conformer was based on the optimum orientation of the donor group (CH_2) for electron delocalization into the π^* orbital of the carbonyl group [18]. The electrostatic interaction between the hydrogens and the oxygen had a minor contribution to the stability [18]. Following the same argument, we interpreted the stability of Ip by considering the long range electrostatic stabilizing interactions between the amino hydrogens and the carbonyl oxygen (2.838 Å) as well as the electron delocalization from the CH_2 group into the π^* orbital of the carbonyl group which mimics the anomeric effect in heteroatom containing cyclic compounds. A comparison of Ip and IIIn indicates that these effects contribute together 1.50 kcal/mol to the stability. Also, the staggered arrangement of the

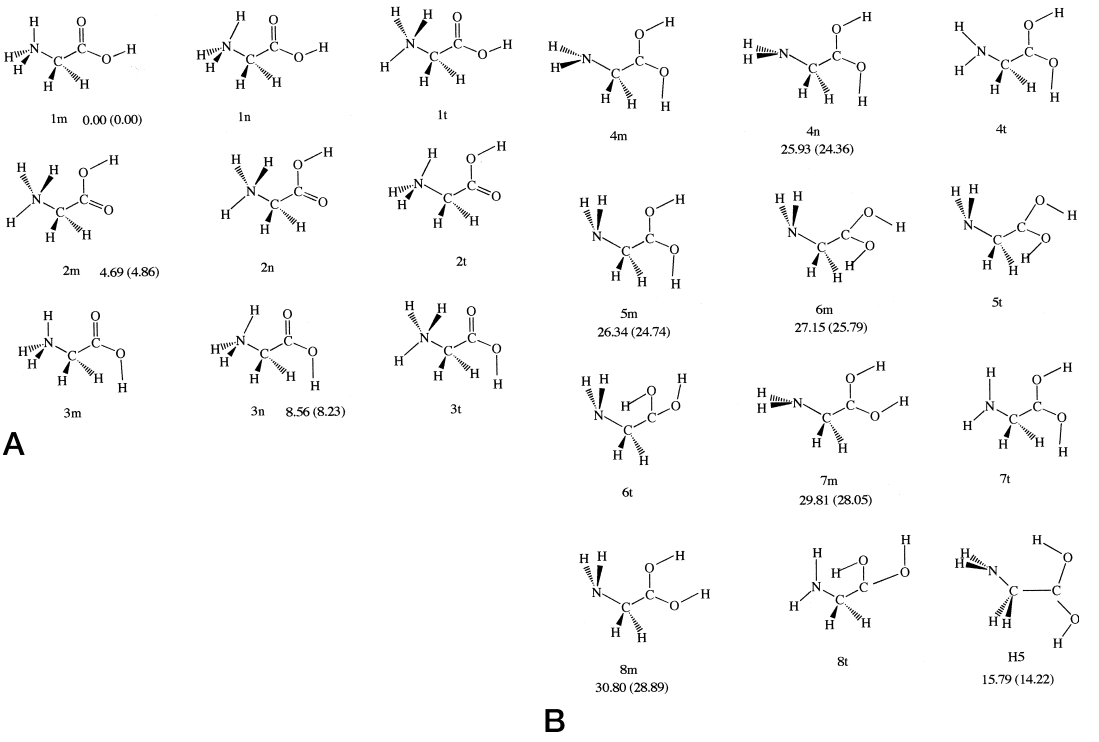

Fig. 2. (a) Conformers of N-protonated glycine; (b) conformers of O-protonated glycine; electronic energies and total energies at 298.15 K are indicated below the structures as $E_{el}(E_{el+thermal})$ in kcal/mol relative to the most stable conformer 1m.

amino protons with respect to the carbonyl carbon reduces the steric effects.

The relative energy of the second glycine conformer, the precursor to the zwitterionic form in solution, IIn, is 0.39 kcal/mol higher in energy with respect to the lowest energy conformer. The structure is stabilized by O–H . . . N type H bonding. The small relative energy indicates that this type of H bonding must be highly stabilizing as it compensates both for the bifurcated NH . . . O=C and C=O . . . H-O interactions. The strong hydrogen bond is countered by a number of unfavorable interactions between the partially eclipsed NH_2 and CH_2 groups, the arrangement of the hydrogen atom of the carboxylic acid group and the orientation of the C–N bond relative to the C=O group. On the other hand, IIp corresponds to a saddle point in accordance with Barone's [19] and Schaefer's [13] findings. Also notice the small energy difference between Ip and IIn with B3LYP/6-31++G** (0.39 kcal/mol) against the value deduced from microwave studies (1.4 ± 0.4). This discrepancy may be an artifact of the method: either the stability of IIn is overestimated or the stability of Ip is underestimated. The length of the N . . . H bond (1.920 Å) and the value of the NCCO torsion angle (4.18°), smaller than the one ascribed by MP2/6-311++G** (10.46°) [20], suggests the formation of a more stable five membered ring in IIn with B3LYP/6-31++G**.

Conformer IIIn (C_1) is 1.50 kcal/mol less stable than Ip. This structure has an extended NCC angle of 119.28°, a consequence of steric repulsion between the NH_2 group and the OH group. The unfavorable arrangement of the methylene group with respect to the carbonyl reduces its stability. Also, the electrostatic interactions of the amino hydrogens with the hydroxyl oxygen are weaker than the ones with the carbonyl oxygen.

Conformer IVn has C_1 symmetry. The O=C–C–N torsion of −21.04° pushes the methylene group in a less favorable orientation with respect to carbonyl for

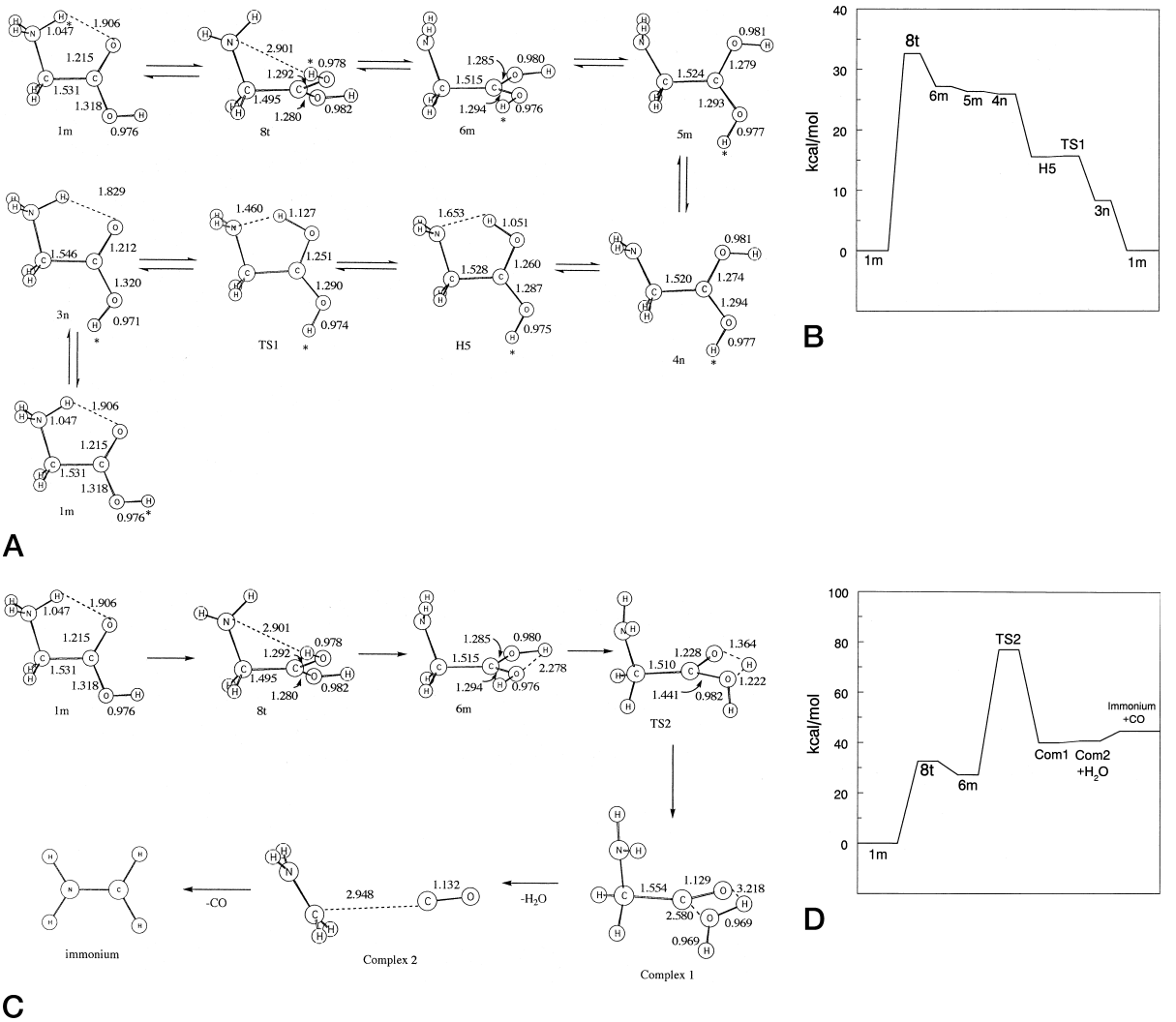

Fig. 3. (a) Reaction mechanism for intramolecular proton migration in protonated glycine. The symbol * indicates the migrating proton. (b) Potential energy profile for proton migration. The symbols 1*m*, 8*t*, 6*m*, etc. correspond to the structures of conformers given in Fig. 2; 8*t* and TS1 are transition states. (c) Reaction mechanism for the unimolecular reaction leading to sequential elimination of H_2O and CO. (d) Potential energy profile for the unimolecular reactions of (c); 8*t* and TS2 are transition states; Com1 and Com2 are complexes 1 and 2, respectively. (e) Mechanism for H_2 elimination from protonated glycine. (f) Potential energy profile for the H_2 elimination from protonated glycine.

electron donation. Instead of the bifurcated arrangement of the amino hydrogens in Ip, in IVn only one hydrogen interacts with the carbonyl oxygen from a shorter distance (2.403 Å) than in Ip (2.838 Å). All these geometrical differences destabilize IVn with respect to Ip by 1.57 kcal/mol. Although conformer IVn is higher in energy than IIIn, it must be noted that inclusion of thermal correction and zero point energy (ZPE) lowers the relative energy of IVn and increases that of IIIn and as a result IVn becomes more stable than IIIn. However, calculated vibrational energies are questionable and will be discussed below.

The differences between Vn and IVn are similar to those between IIIn and Ip, i.e. the orientation of the carbonyl group with respect to amino and methylene groups. Vn is less stable than IVn by 1.16 kcal/mol, a

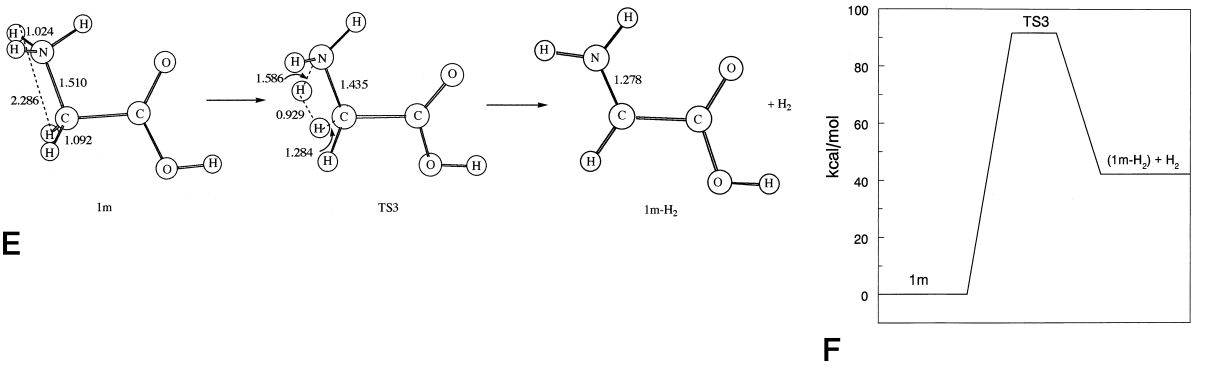

Fig. 3. (Continued)

value comparable to the relative energy of IIIn with respect to Ip (1.50 kcal/mol). On the other hand, the H–N–C–C torsion angle in Vn (60.07°) is larger than the one in IVn (40.06°) and the N–H . . . O–C distance is longer (2.456 Å), a consequence of the reduced electrostatic interaction of the hydrogen with the less electronegative hydroxyl oxygen.

Conformer VIp differs from Ip in having an anti orientation of the acidic OH group. The energy difference (5.75 kcal/mol) represents the strength of the C–O . . . H–O interaction.

Conformer VIIIn is the highest energy conformer lacking the most stabilizing H-bonding interactions. It is similar to VIp in the anti orientation of the carboxyl group and also similar to IVn in the orientation of the carbonyl with respect to amino group. Its relative energy with respect to Ip (7.38 kcal/mol) is comparable to the sum of the relative stabilities of IVn and VIp (7.32 kcal/mol).

The “B type” H bonding seems to be the strongest interaction since it compensates the effects of the various unfavorable orientations. The “A type” H bonding has also a very important stabilizing effect.

As shown in Table 2, B3LYP/6-31++G** energies are in reasonable agreement with the MP2/6-311++G** [20] energies whereas HF/6-31G* [9] predicts a different order of stability. The B3LYP/6-31++G** method performed significantly better than the HF method [9] and almost as well as the high level ab initio methods (CISD [13], CCSD [13], MP2 [20]) for bonded distances (Table 1). But, the nonbonded N–H . . . O–C distances in the bifurcated arrangements are longer by about 0.05 Å than those found in the correlated ab initio treatments. On the other hand, the O–H . . . N distance in IIn is lower by about 0.02–0.05 Å and the N–C–C–O torsion angle is smaller by about 10°. These observations suggest that B3LYP/6-31++G** over stabilizes the latter type of interaction whereas it underestimates the stability of the bifurcated arrangements. This fact is reflected in the relative stability of IIn. Another problem is that the conformer VIIp obtained by Császár [20] does not exist on the B3LYP/6-31++G** potential energy surface. Since this species exists in Barone’s [19] DFT work, its absence can be considered to result from the use of a different basis set.

The vibrational frequencies are very sensitive to the method of choice. For instance, the lowest frequency vibrations in Ip, IIn, and IIIn are 60, 14, and 27 cm^{-1}, respectively, in our calculations. The same vibrational modes are 54, 79, and 86 cm^{-1} with the MP2/6-311++G** method [20,32] and 72, 87, and 16 cm^{-1} with the HF/DZP method [13], respectively. This point was also noted by Hagler and co-workers [32]. In addition, the harmonic approximation may not be a suitable method for the vibrations where the energy exceeds the barrier (in IIn and IIIn). There is experimental evidence that the most abundant glycine conformer is Ip [24] but a Boltzmann distribution based on the calculated Gibbs free energies in this study suggests that IIn has a higher population at 298 K. This seems to be due to the errors in the calculation of the vibrational contributions to the free energy.

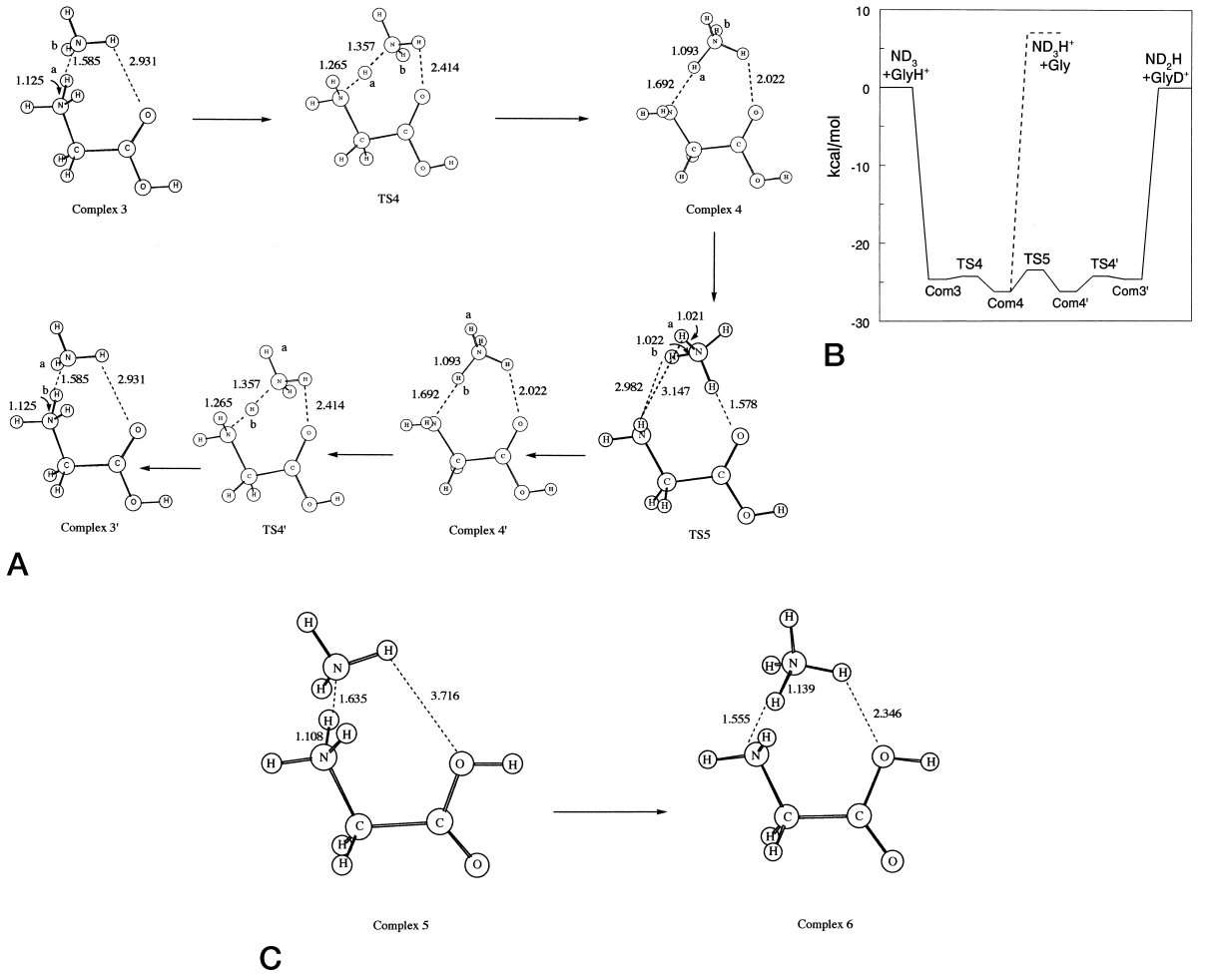

Fig. 4. (a) Exchange mechanism of the amine proton of N-protonated glycine (1*m*) with ammonia. Protons a and b are the ones involved in the exchange. Primed structures are the same as the unprimed ones except for isotopic exchange. (b) Potential energy profile for the proton exchange reaction of the amine proton with ammonia and for proton transfer from the amine proton to ammonia; Com 3, 3′, 4 and 4′ are the complexes of (a); TS4, TS4′ and TS5 are the transition state structures of (a). (c) Isomerization from the ion/dipole complex to a hydrogen bonded ammonium complex in the case of the 2*m* conformer of N-protonated glycine. (d) Mechanism of exchange of the carboxylic proton of N-protonated glycine (1*m*) with ammonia. Protons a and b are the ones involved in the exchange. The primed structure is the same as the unprimed one except for isotopic exchange. (e) Potential energy profiles, (i) for H/D exchange of the carboxylic proton of N-protonated glycine with ammonia; (ii) for proton transfer to ammonia from the carboxylic position of N-protonated glycine; Com 7, 7′ and 8 are the complexes whose structures are given in (d) and (f) mechanism of transfer of the carboxylic proton from N-protonated glycine to ammonia. Complex 7 is a salt bridge structure whereas complex 8 is an ion/dipole complex between the ammonium ion and the IIn conformer of neutral glycine.

Therefore, we suspect that the vibrational energies obtained in our calculations include some inaccuracy.

3.2. Protonated glycines

In glycine, there are three basic sites for protonation: the nitrogen and the two oxygen atoms. Calculations showed that the most basic site is the amino nitrogen [14,33,34]. Campbell et al. [35] used experimental lone pair ionization energies to identify the nitrogen as the protonation site. Theoretical investigations of Bouchonnet and Hoppilliard [33] indicated that protonation at the hydroxyl oxygen led to decomposition and formation of an ion dipole complex.

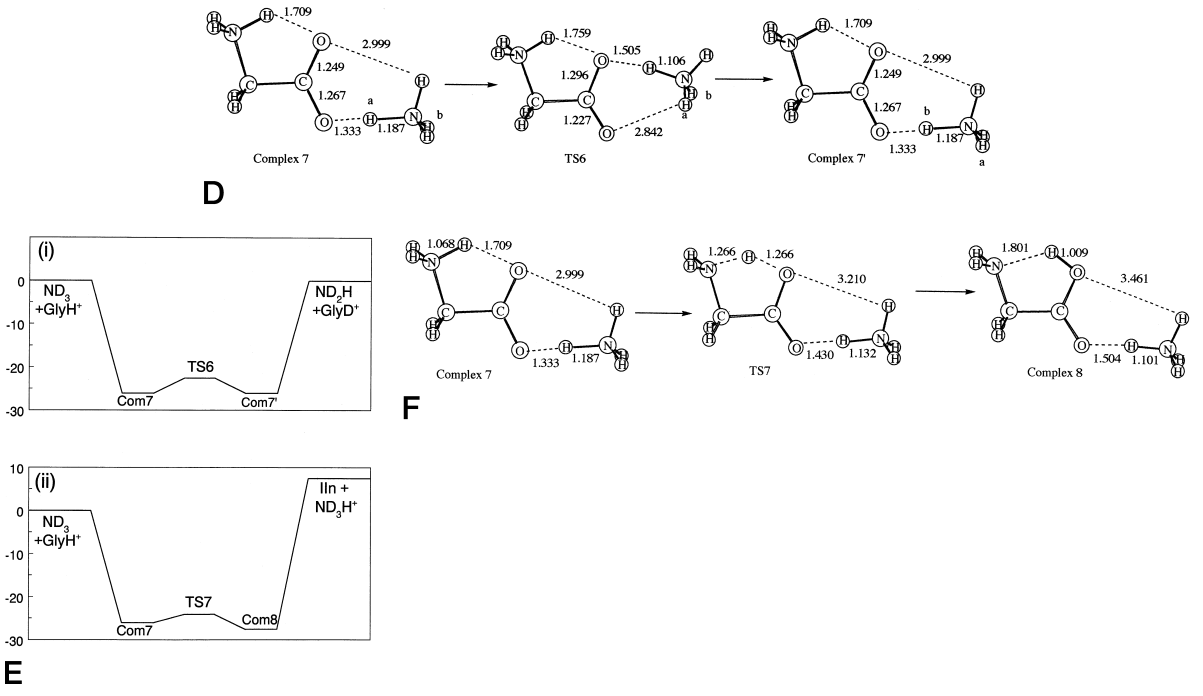

Fig. 4. (Continued)

Several semiempirical [3] and ab initio (HF [33,34], MP2 [14], G2(MP2) [36]) calculations appeared in the literature. The most complete study was that of Zhang and Chung-Phillips [14] where they optimized 9 N-protonated and 11 O-protonated species (both minima and saddle points) at the MP2 level of theory. In Fig. 2 these structures are presented with the addition of a HF structure by Jensen (H5) [34]. The subscripts *m* and *t* stand for minimum and transition state respectively, the subscripts n represent the transition structures which are satellite species of the minima. This nomenclature is adopted from Zhang and Chung-Phillips [14] and our minima do not necessarily correspond to minima in their study. Semiempirical methods [3] and HF theory [34] have predicted 1*t* as the most stable protonated glycine structure whereas at the MP2 level of theory [14] it was identified as a transition state and 1*m* was located as the global minimum (Fig. 2). Moreover, two of the HF species did not exist at all at the MP2 level [14]. These observations underline the importance of the correlated level optimizations. Experiments on protonated glycine focused on the proton affinity (PA) and gas phase basicity (GB). Using the kinetic method, Wu and Fenselau [37] obtained a PA of 211.6 kcal/mol. Bracketing experiments by Wu and Lebrilla [3] and Zhang et al. [8] yielded 215.4 and 213.5

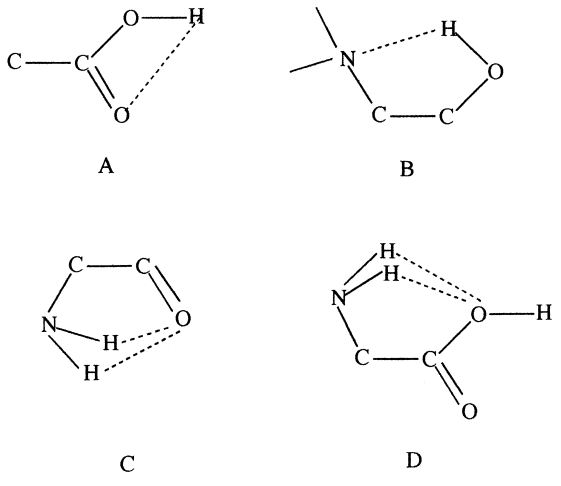

Scheme 1. Types of intramolecular hydrogen bonds formed by different conformers of glycine.

kcal/mol, respectively. These PA values indicate that protonation mainly occurs at the amino site. In their MP2 calculations, Zhang and Chung-Phillips showed that BSSE and conformational equilibrium effects were important for an accurate evaluation of GB [21].

3.2.1. N-protonated glycines

Three different conformers were located in our calculations as minima on the potential energy surface of protonated glycines. These structures correspond to 1*m*, 2*m* and 3*n* of Zhang and Chung-Phillips [14] and are displayed in Fig. 2(a). Structures 1*m* and 2*m* have C_1 symmetry whereas 3*n* belongs to the C_s point group. With the MP2/6-311+G** calculations 3*n* turned out to be a saddle point and the corresponding minimum 3*m* has C_1 symmetry; the small energy difference disappeared upon inclusion of zero point energies [14]. We did not attempt to locate a similar structure with C_1 symmetry. On the other hand, the species located as a minimum with AM1 [3] and HF/6-31G* [34] and also by our preliminary AM1 and PM3 results corresponds to 1t (Fig. 2). It is identified as a rotational transition state both by MP2/6-311+G** and by our present B3LYP/6-31++G** calculations. It seems that AM1 and HF/6-31G* do not treat correctly the strength of the single hydrogen bond N–H . . . O–C, instead they favor a bifurcated H-bonded arrangement where the carbonyl carbon assumes a gauche conformation with respect to the amino hydrogens reducing the steric repulsion.

The geometrical parameters for the compounds studied are displayed in Table 3. The energetics of the protonated glycine conformers is presented in Table 5. For comparison, MP2 energies of Zhang and Chung-Phillips [14] are also given in the same table. All the bond lengths in the three species, except for one N–H bond length in 1*m*, are generally 0.005 Å longer than the ones calculated with MP2/6-311+G**. On the other hand, in 1*m*, the bond length of the H atom involved in H bonding is 1.047 Å whereas it is 1.033 Å at MP2/6-311+G** level [14]. The H-bond distance is 1.906 Å at the B3LYP/6-31++G** level but 2.074 Å at MP2/6-311+G** [14]. This fact shows that the attraction between O and H is stronger at the B3LYP/6-31++G** level. On the other hand, the bifurcated H bond in 2*m* is longer at the B3LYP/6-31++G** level. The H-bonding distances in both calculations agree with each other for 3*n*. The relative energy of 2*m* is higher with B3LYP/6-31++G**, than the one calculated with MP2/6-311+G**, whereas the relative energy of 3*n* is lower than its counterpart with MP2/6-311+G**. These observations suggest that the N–H . . . O=C single H bond is stronger with B3LYP than with MP2 whereas the bifurcated bond is weaker. Also, the C=O . . . H–O interaction seems to be weaker with B3LYP.

The observed geometries and stabilities may be explained by the strength of the intramolecular H bonding. In 1*m*, the strength of the NH . . . OC interaction overcomes the steric repulsion due to the eclipsed conformation of the amino group and the adjacent carbon. In 2*m*, the CO and amino groups are trans to each other. The amino hydrogens are under the effect of the less electronegative hydroxyl oxygen which is not enough to overcome the steric repulsion and a gauche conformation resulting in a bifurcated H bonding is favored. Since this interaction is weaker, 2*m* is less stable than 1*m*. In 3*n*, the O–H . . . O=C interaction is missing, a fact that destabilizes this conformer with respect to 1*m* and 2*m*. A single H bond rather than a bifurcated one is preferred for similar reasons as in 1*m*. The most important consequence of protonation in all the three conformers with respect to the neutral one is the increase in the C–N bond length (about 0.06 Å). This indicates that protonation is also assisted by the electrons of the C–N bond, which shift toward the nitrogen atom.

3.2.2. O-protonated glycines

Six different conformers of O-protonated glycines at the carbonyl O were located as stationary points and identified as minima by their real vibrational frequencies [Fig. 2(b)]. Four of these structures, 4*n* (C_s), 6*m* (C_1), 7*m* (C_s), 8*m* (C_s) correspond to those found in the MP2/6-311+G** calculations of Zhang and Chung-Phillips [14]. The structure 4*n* found by Zhang and Chung-Phillips is a transition structure, the corresponding minimum, 4*m*, has C_1 symmetry and the difference in energy is insignificant

[14]. Similarly, we located a structure very similar to 5*m* (C_s), belonging to the C_1 point group; we named this conformer 5*m*. The sixth structure which has the lowest relative energy at the B3LYP/6-31++G** level, corresponds to the one obtained in HF/6-31G* calculations of Jensen [34] and is named H5. As will be discussed later, the thermal energy of H5 exceeds the barrier separating it from 1*m* and the O-protonated species collapses to the N-protonated one. Therefore, the difference between MP2 and B3LYP results is physically insignificant. Another HF/6-31G* species, H4 [34], does not exist at either the B3LYP/6-31++G** or the MP2/6-311+G** levels [14]. The latter species has however been identified as a stationary point with our preliminary AM1 and PM3 calculations. The difference between HF/6-31G* and B3LYP/6-31++G** results can be explained by the effect of electron correlation.

The relative stabilities of the O-protonated glycine conformers are governed by intramolecular H bonding as well as by steric effects. The intramolecular H bonding in H5 makes it the most stable O-protonated conformer. In all the conformers, the most important destabilizing factor is the syn–syn conformation of the two geminal hydroxyl groups. Conformers 8*m* and 7*m* differ from 5*m* and 4*n* by the conformation of the geminal hydroxyl groups, respectively. The difference between the two conformations of the hydroxyl groups is about 4 kcal/mol in both cases. The relative stability of the syn–anti conformation arises from the lack of steric repulsion between the hydroxyl hydrogens as well as the H bonding between OH . . . OH. Another factor affecting the stability is the conformation of the amino group. In the O-protonated conformers, there is no carbonyl group, therefore no stability is gained with a favorable orientation of the methylene group and as observed with the neutral conformers the bifurcated H bonding is very weak. In the conformers where the two amino hydrogen atoms are directed towards the hydroxyl (5*m* and 8*m*) the destabilizing effect of steric repulsion between hydrogens and the carbon is higher than the stability gained from the bifurcated H bonding. However, when these hydrogens are directed “outside” there is no steric repulsion. Therefore 7*m* and 4*n* are more stable than 8*m* and 5*m* by 0.85 and 1.43 kcal/mol, respectively. The intramolecular H bonding and the conformations of the OH and amino groups result in a stability order as follows: H5 > 4*n* > 5*m* > 6*m* > 7*m* > 8*m*. This order is similar to the one produced with MP2/6-311+G** [14] although the relative energies are 2.5–3 kcal/mol smaller than the ones calculated with MP2/6-311+G**.

Since the amino N is more basic than the carbonyl O, O-protonated species are much less stable than the N-protonated ones. The most important geometric change occurs at the CO bond length upon O-protonation. Since the carbonyl group is converted to COH, both CO bond lengths become closer to each other, having partial double bond character. In H5, because of the N . . . HO intramolecular H bonding, the N–H and C–N bonds are longer than in the other O-protonated conformers. Similarly, in the conformers having syn-anti conformation of the OH groups, the OH and CO bond lengths of the atoms, which are not involved in H bonding, are shorter than the other ones.

Our geometrical parameters and the MP2/6-311+G** results [14] (for the species that exist at both levels) are usually in agreement within 0.005 Å. The most important difference is in the C–C bond lengths which are systematically shorter by about 0.01 Å at the MP2/6-311+G** level.

3.3. Unimolecular reactions

In an early work on the fragmentation of amino acids, Tsang and Harrison [38] observed the loss of the elements of formic acid in the CH_4 chemical ionization (CI) mass spectrum of glycine. They attributed this to the sequential elimination of water and CO. In the H_2 CI spectrum, the loss of H_2 was also observed, HCOOH elimination still being the major fragmentation channel. Later, in addition to the above channels Bouchonnet et al. [39] detected the elimination of CO_2 and further fragmentation of the daughter ion resulting from HCOOH elimination using plasma desorption mass spectrometry. Different proposals were made for the relationship between the site of protonation and the fragmentation mechanism. One

possibility was that fragmentation occurred at the site of protonation. Another suggestion was that protonation occurred at the most basic site, then the proton migrated to the carboxyl group. A third approach was that protonation occurred at any site and complete randomization of protons took place before fragmentation. Recently, Harrison and Yalçın [40] indicated that the labile protons are very mobile in some amino acids and small peptides, supporting the third approach.

3.3.1. Proton migration

Starting with the most stable protonated glycine (1*m*) proton migration is depicted in Fig. 3(a). The corresponding potential energy profile is presented in Fig. 3(b). The step that requires the most energy is the one in which a proton migrates from nitrogen to the carbonyl oxygen (1*m*---8*t*). Structure 8*t* is a transition state lying 32.59 kcal/mol (30.80 kcal/mol with the inclusion of thermal contributions) above 1m and goes downhill to 6m. We did not optimize the transition structures in the conformational interconversions of the O-protonated species. According to Zhang and Chung-Phillips [14] these barriers are small. The rearrangement through 5*m*, 4*n*, H5, 3*n* to 1*m* is always downhill and H5 and TS1 do not exist in the MP2 results of [14]. On the other hand, in our calculations, the thermal energy exceeds the barrier (0.14 kcal/mol) represented by TS1 therefore H5 and 3n become indistinguishable. The mechanism proposed in Fig. 3(a) indicates that, no matter what the initial protonation site is, the proton can migrate throughout the molecule if the system has an energy greater than a threshold of 32.6 kcal/mol. This threshold was found to be 33.35 kcal/mol with MP2/6-311+G** method by Zhang and Chung-Phillips [41]. This is consistent with Harrison's observation [40] indicating that there is complete scrambling of protons in many protonated amino acids. Whereas there may be other intramolecular proton migration channels, the one presented in Fig. 3(a) and (b) seems to be energetically the most favorable.

3.3.2. Fragmentation reaction

Protonation at the hydroxyl oxygen results in the decomposition of the molecule [33]. An ion–dipole complex of water and the resulting acylium ion is observed. Besides direct protonation of the hydroxyl oxygen, intramolecular proton migration may bring the proton to that position and result in fragmentation. Starting with the most stable conformer of protonated glycine 1m, the fragmentation reaction is realized after migration of a proton from the N terminus to the carbonyl oxygen [Fig. 3(c)]. The conversion of 1*m* to 6*m* is identical to the one in the proton migration reaction [Fig. 3(a) and (b)]. The full fragmentation energy profile is represented in Fig. 3(d). As much as 49.75 kcal/mol (45.82 kcal/mol with the thermal contributions) are needed in order for structure 6*m* to fragment as seen in the 6*m*→TS2 transition. Provided that 50 kcal/mol are gained by the O protonated glycine an ion–dipole complex (complex 1) will form. The acylium ion is only stable when solvated. The evaporation of water from complex 1 leads to further fragmentation to an ion–dipole complex of an immonium ion and carbon monoxide (complex 2). This process is endothermic by 0.63 kcal/mol when one considers only the electronic energies but exothermic by −1.52 kcal/mol with the inclusion of the thermal contributions, reflecting the well-known high stability of the immonium ion. Finally, carbon monoxide evaporates leaving the immonium ion as the ionic fragment. This fragmentation pattern depicts the experimental findings of Tsang and Harrison [38] who observed the loss of the elements of formic acid and attributed it to the sequential loss of water and carbon monoxide.

Another fragmentation channel is the elimination of H_2 [Figs. 3(e) and (f)]. The barrier for the fragmentation is 91.58 kcal/mol (85.50 kcal/mol with the inclusion of the thermal contributions), a value much higher than the barrier for the sequential elimination of H_2O and CO. $PA(H_2)$ = 101.2 kcal/mol [42]. If PA(Gly) = 211.6 kcal/mol [37], proton transfer from H_3^+ to glycine is 110.4 kcal/mol exothermic whereas since $PA(CH_4)$ = 131.6 kcal/mol, proton transfer from CH_5^+ to Gly is only 80.0 kcal/mol exothermic. Therefore, since H_2 CI is more exothermic than CH_4

CI, H_2 elimination is only observed in the former case [38].

3.4. Bimolecular reactions

There exist four labile protons in protonated glycine, three at the amino site and one at the carboxylic site. Campbell et al. [2] investigated the H/D exchange reactions of glycine and its oligomers with D_2O, CD_3OD, CD_3CO_2D, and ND_3 in mass spectrometric experiments supported by semiempirical calculations. For glycine, they observed that D_2O exchanged one labile proton whereas the other bases exchanged all four labile protons. They also observed that ND_3 could make multiple proton exchanges in a single collision. They proposed an 'onium' mechanism for the exchange of amino protons and a salt bridge complex formation for the carboxylic proton.

3.4.1. Exchange of the amino protons [Fig. 4(a) and (b)]

Ammonia approaches both the carbonyl oxygen and the $-NH_3^+$ end of the molecule (complex 3). The H-bonding distances are 1.585 Å for the H . . . N bond between the nitrogen atom of ammonia and the hydrogen of the $GlyH^+$. The hydrogen of ammonia is 2.931 Å away from the carbonyl oxygen. The transfer of the proton from $GlyH^+$ to NH_3 has a barrier of 0.36 kcal/mol when only the electronic energies are considered. On the other hand, when thermal contributions are also included the energy exceeds the barrier. TS4 becomes more stable than complex 3 by −2.16 kcal/mol. In fact, this negative number has no quantitative meaning but indicates that the two minima are physically indistinguishable. Therefore, the sequence complex 3, TS4 and complex 4 illustrates the motion of the proton oscillating back and forth between glycine and ammonia. Regarding the PA difference between NH_3 and Gly (about 7–8 kcal/mol), one might expect this process of intramolecular proton transfer to require a higher barrier but there is a compensating effect of H bonding between NH_3 and the carbonyl group. TS5 corresponds to the rotation of NH_4^+ around itself resulting in a barrier of 2.79 kcal/mol (2.29 kcal/mol with the thermal corrections). After the rotation, a proton different than the one taken from $GlyH^+$ is oriented towards the amino group. This mechanism may be repeated before ammonia leaves complex 3 and results in multiple proton exchanges provided the amino group rotates around itself and gives another proton to ammonia. This mechanism is in agreement with the onium mechanism proposed for H/D exchange between ND_3 and $GlyH^+$ by Campbell et al. [2]. The corresponding potential energy profile is shown in Fig. 4(b).

The most stable protonated glycine is 1*m* and conformer 2*m* is too high in energy to coexist with 1*m* to a considerable amount. Yet, it is interesting to see how the proton exchange occurs with 2*m* where the amino group assumes a trans conformation with respect to carbonyl [Fig. 4(c)]. The transition from complex 5 to complex 6 is endothermic by 1.56 kcal/mol (1.11 kcal/mol with the inclusion of the thermal contributions), contrary to the case of 1*m*. A comparison of Fig. 4(a) and (c) shows that the distance of the ammonia and ammonium protons to the hydroxyl oxygen of 2*m* is larger than the one to the carbonyl oxygen of 1m. This fact indicates that multiple hydrogen bonding which facilitates the proton transfer is very weak or nonexistent with 2*m*. The proton exchange reaction at the amino site with 2*m* is expected to be slower than the one with 1*m*.

3.4.2. Exchange of the carboxylic proton [Figs. 4(d) and 4(e)]

Approach of ammonia to the carboxylic end of the molecule produces complex 7, which can be considered as a zwitterionic glycine solvated by an ammonium ion. There are two nonbonded interactions between the ammonium protons and glycine oxygens. One of these nonbonded distances seems to be too large (2.999 Å) and the other too short (1.333 Å). These may be artifacts of the computational method used. On the other hand a Mulliken population analysis shows that charge separation occurs and complex 7 can be considered as a salt-bridged structure. One ammonium molecule is enough to solvate and to stabilize the zwitterionic glycine. Once complex 7 is formed, NH_4^+ may rotate and transfer to the glycine a proton different from the one originally captured. This

mechanism is in agreement with the one suggested by Campbell et al. [2] but we did not find with our level of calculation the ion/dipole complex ($GlyH^+ \ldots NH_3$) that they propose. The potential energy profile for hydrogen deuterium exchange at the carboxyl is presented in Fig. 4(e), part (i). The barrier for the exchange of the carboxyl proton, including thermal energy, (complex 7---TS6, 4.42 kcal/mol) is higher than the one for the amino proton (complex 4---TS5, 2.29 kcal/mol). This may account for the difference in the experimental reaction rates at the two sites.

The exchange of the carboxylic proton of 2m is also expected to proceed via a salt bridge mechanism. The transition state and product are expected to be identical to the ones occurring for 1m.

3.4.3. Proton transfer from protonated glycine to ammonia [Fig. 4(a), (b), (e), and (f)]

Proton transfer from the amino site of protonated glycine to ammonia may occur by the evaporation of NH_4^+ from complex 4 of Fig. 4(a), also shown in the potential energy profile in Fig. 4(b).

The transfer of the carboxylic proton to ammonia occurs via a salt bridge (complex 7). A low barrier proton transfer through TS7 may lead to complex 8 and the evaporation of NH_4^+ leaves glycine IIn. These reaction steps are presented in Fig. 4(f) and the corresponding energetics in the potential energy profile of Fig. 4(e), part (ii).

Both proton transfer processes are endothermic by about 7–8 kcal/mol and this value corresponds to the PA difference between NH_3 and Gly.

4. Conclusion

Conformers of the neutral, N-protonated and O-protonated glycines were investigated at the B3LYP/6-31++G** level of theory. This method was found to perform better than the HF method and as well as the high level ab initio methods in most cases. B3LYP resulted in stronger single H bonds and weaker bifurcated arrangements with respect to MP2 and higher level methods.

Seven neutral, three N-protonated and six O-protonated species were located as minima. Different types of hydrogen bonds, steric repulsion and the orientation of the methylene group with respect to the carbonyl explain the relative stabilities of these structures.

Although the most basic site is the amino position, the proton can migrate to the carbonyl position if it can pass over a barrier of ~33 kcal/mol in the protonated glycine. On the other hand, overcoming a barrier of 50 kcal/mol may lead to fragmentation. In this case, the proton migrates to the hydroxyl oxygen resulting in an ion–dipole complex. Further fragmentation follows the evaporation of water and a new ion–dipole complex is formed. This mechanism is in agreement with the sequential loss of water and carbon monoxide observed experimentally.

There exist four labile protons in protonated glycine. The amino protons are exchanged by an onium mechanism and the carboxylic proton is exchanged via the formation of a salt bridge complex. The central barrier for the latter reaction in a double well potential energy profile is slightly higher than the former one.

Acknowledgement

This research was supported by the Boğaziçi University Araştırma Fonu (project no. 99B504D) and by The Israel Science Foundation founded by the Israel Academy of Sciences and Humanities. The Farkas Research Center is supported by the Minerva Gesellschaft für die Forschung GmbH, München.

References

[1] C. Lifshitz, G. Koster, Int. J. Mass Spectrom. 182/183 (1999) 213.
[2] S. Campbell, M.T. Rodgers, E.M. Marzluff, J.L. Beauchamp, J. Am. Chem. Soc. 117 (1995) 12840.
[3] J. Wu, C.B. Lebrilla, J. Am. Chem. Soc. 115 (1993) 3270.
[4] E. Gard, D. Willard, J. Bregar, M.K. Green, C.B. Lebrilla, Org. Mass Spectrom. 28 (1993) 1632.
[5] D. Suckau, S. Yueer, S.C. Beu, M.W. Senko, J.P. Qiunn, F.M. Wampler III, F.W. McLafferty, Proc. Natl. Acad. Sci. USA 90 (1993) 790.

[6] X. Cheng, C. Fenselau, Int. J. Mass Spectrom. Ion Processes 122 (1992) 109.
[7] E.H. Gur, L.J. Konning, N.M.M. Nibbering, J. Am. Soc. Mass Spectrom. 6 (1995) 466.
[8] K. Zhang, D.M. Zimmerman, A. Chung-Phillips, C.J. Cassidy, J. Am. Chem. Soc. 115 (1993) 10812.
[9] J.H. Jensen, M.S. Gordon, J. Am. Chem. Soc. 113 (1993) 7917.
[10] K. Zhang, C.J. Cassidy, A. Chung-Phillips, J. Am. Chem. Soc. 116 (1994) 11512.
[11] R.F. Frey, J. Coffin, S.Q. Newton, M. Ramek, V.K.W. Cheng, F.A. Momany, L. Schäfer, J. Am. Chem. Soc. 114 (1992) 5369.
[12] M. Ramek, F.A. Momany, D.M. Miller, L. Schäfer, J. Mol. Struct. 375 (1996) 189.
[13] C. Hu, M. Shen, H.F. Schaefer III, J. Am. Chem. Soc. 115 (1993) 2923.
[14] K. Zhang, A. Chung-Phillips, J. Comput. Chem. 19 (1998) 1862.
[15] A.D. Becke, J. Chem. Phys. 98 (1993) 5648.
[16] C. Lee, W. Yang, R.G. Parr, Phys. Rev. B 37 (1988) 785.
[17] E.F. Strittmatter, E.R. Williams, Int. J. Mass Spectrom. 185/186/187 (1999) 935.
[18] D. Yu, D.A. Armstrong, A. Rauk, Can. J. Chem. 70 (1992) 1762.
[19] V. Barone, C. Adamo, F. Lelj, J. Chem. Phys. 102 (1995) 364.
[20] A.G. Császár, J. Am. Chem. Soc. 114 (1992) 9568.
[21] K. Zhang, A. Chung-Philips, J. Phys. Chem. A 102 (1998) 3625.
[22] (a) R.D. Suenram, F.J. Lovas, J. Mol. Spectrosc. 72 (1978) 372; (b) L. Schäfer, H.L. Sellers, F.J. Lovas, R.D. Suenram, J. Am. Chem. Soc. 102 (1980) 6566; (c) R.D. Suenram, F.J. Lovas, ibid. 102 (1980) 7180.
[23] (a) R.D. Brown, P.D. Godfrey, J.W.V. Storey, M.P. Bassez, J. Chem. Soc., Chem. Commun. (1978) 547; (b) P.D. Godfrey, R.D. Brown, J. Am. Chem. Soc. 117 (1995) 2019.
[24] K. Iijima, K. Tanaka, S. Onuma, J. Mol. Struct. 246 (1991) 257.
[25] S.G. Stepanian, I.D. Reva, E.D. Radchenko, M.T.S. Rosado, M.L.T.S. Duarte, R. Fausto, L. Adamowicz, J. Phys. Chem. A 102 (1998) 1041.
[26] GAUSSIAN 94, Revision C.2, M.J. Frish, G.W. Trucks, H.B. Schlegel, P.M.W. Gill, B.G. Johnson, M.A. Robb, J.R. Cheesman, T. Keith, G.A. Petersson, J.A. Montgomery, K. Raghavachari, M.A. Al-Laham, V.G. Zakrzewski, J.V. Ortiz, J.B. Foresman, J. Cioslowski, B.B. Stefanov, A. Nanayakkara, M. Challacombe, C.Y. Peng, P.Y. Ayala, W. Chen, M.W. Wong, J.L. Andres, E.S. Replogle, R. Gomperts, R.L. Martin, D.J. Fox, J.S. Binkley, D.J. Defrees, J. Baker, J.J.P. Stewart, M. Head-Gordon, C. Gonzales, J.A. Pople, Gaussian Inc., Pittsburgh, PA, 1995).
[27] J.J.P. Stewart, J. Comput. Chem. 10 (1989) 209; 10 (1989) 221.
[28] SPARTAN, Version 4.0 Wavefunction, Inc. 18401 Von Karman Ave., 370 Irvine, CA 92715, USA.
[29] J.E. Del Bene, W.B. Person, K. Szczepaniak, J. Phys. Chem. 99 (1995) 10705.
[30] P.D. Godfrey, R.D. Brown, F.M. Rodgers, J. Mol. Struct. 376 (1996) 65.
[31] I.D. Reva, A.M. Plokhotnichenko, S.G. Stepanian, A.Y. Ivanov, E.D. Radchenko, G.G. Sheina, Y.P. Blagoi, Chem. Phys. Lett. 232 (1995) 141; Erratum, 235 (1995) 617.
[32] D.T. Nguyen, A.C. Scheiner, J.W. Andzelm, S. Sirois, D.R. Salahub, A.T. Hagler, J. Comput. Chem. 18 (1997) 1609.
[33] S. Bouchonnet, Y. Hoppilliard, Org. Mass Spectrom. 27 (1992) 71.
[34] F. Jensen, J. Am. Chem. Soc. 114 (1992) 9533.
[35] S. Campbell, J.L. Beauchamp, M. Rempe, D.L. Lichtenberger, Int. J. Mass Spectrom. Ion Processes 117 (1992) 83.
[36] D. Yu, A. Rauk, D.A. Armstrong, J. Am. Chem. Soc. 117 (1995) 1789.
[37] Z. Wu, C. Fenselau, J. Am. Soc. Mass Spectrom. 3 (1992) 863.
[38] C.W. Tsang, A.G. Harrison, J. Am. Chem. Soc. 98 (1976) 1301.
[39] S. Bouchonnet, J.P. Denhez, Y. Hoppilliard, C. Mauriac, Anal. Chem. 64 (1992) 743.
[40] A.G. Harrison, T. Yalçın, Int. J. Mass Spectrom. Ion Processes 165 (1997) 339.
[41] K. Zhang, A. Chung-Phillips, J. Chem. Inf. Comput. Sci. 39 (1999) 382.
[42] S.G. Lias, J.E. Bartmess, J.F. Liebman, J.L. Holmes, R.D. Levin, W.G. Mallard, J. Phys. Chem. Ref. Data 17 (1988) (suppl. no 1).